Article

Solvent Influence in the Synthesis of Lead(II) Complexes Containing Benzoate Derivatives

José A. Ayllón [1],*, Oriol Vallcorba [2] and Concepción Domingo [3]

1   Departament de Química, Universitat Autònoma de Barcelona, 08193 Bellaterra, Spain
2   ALBA Synchrotron Light Source, 08290 Cerdanyola del Vallés, Spain; ovallcorba@cells.es
3   Instituto de Ciencia de Materiales de Barcelona (CSIC), 08193 Bellaterra, Spain; conchi@icmab.es
*   Correspondence: joseantonio.ayllon@uab.es

Abstract: A series of lead(II) complexes incorporating benzoate derivative ligands was prepared: $[Pb(2MeOBz)_2]_n$ (**1**), $[Pb(2MeOBz)_2(H_2O)]_n$ (**2**), $[Pb_2(1,4Bzdiox)_4(DMSO)]_n$ (**3**), $[Pb(1,4Bzdiox)_2(H_2O)]_n$ (**4**), $[Pb(Pip)_2(H_2O)]_n$ (**5**), and $[Pb(Ac)(Pip)_2(MeOH)]_n$ (**6**) (2MeOBz: 2-methoxybenzoate; 1,4Bzdiox: 1,4-benzodioxan-5-carboxylate; DMSO: dimethylsulfoxide; Ac: acetate; Pip: piperonylate; MeOH: methanol). All compounds were characterized via elemental analysis, ATR-FTIR spectroscopy, and powder XRD. In addition, the crystal structures of some compounds were elucidated. Compounds **1** and **2**, involving 2-methoxybenzoate, were closely related, only differing in the presence of one extra aqua ligand found for the latter. However, this implies key changes in the studied properties, e.g., **2** shows solid-state luminescence that displays a different color as a function of the crystal orientation, while **1** does not. The crystal structure of **2** revealed a 1D coordination polymer. A similar relationship was found between compounds **3** and **4**, incorporating 1,4-benzodioxan-5-carboxylate. In this pair, only **4**, with aqua ligands, displayed a greenish-yellow-color solid-state luminescence. Furthermore, two new lead(II) piperonylate complexes, **5** and **6**, were obtained from the reaction between lead(II) acetate and piperonylic acid. In water, all acetate ligands in the metal precursor were displaced and $[Pb(Pip)_2(H_2O)]_n$ (**5**) was isolated, while in methanol, a mixed acetate–piperonylate complex, $[Pb(Ac)(Pip)_2(MeOH)]_n$ (**6**), was precipitated. Considering only conventional Pb-O bonds, the crystal structure of **6** was described as a 1D coordination polymer, although, additionally, the chains were associated via tetrel bonds, defining an extended 2D architecture.

Keywords: Pb(II) complexes; coordination polymers; supramolecular networks; photoluminescence; tetrel bonds

1. Introduction

There are many reasons to study the coordination chemistry of Pb(II), highlighting that a proper knowledge of the Pb(II) coordination properties is crucial for the understanding of the toxicological properties of the cation [1], but also to improve the knowledge for applying its complexes as luminescent compounds [2–5] or nonlinear optical materials [5–7], or to study new precursors for bulk or nanostructured PbS and PbSe [8,9]. Chemically, Pb(II) shows a high degree of tolerance for ligand coordination in regard to potential geometries and attained bond lengths, rarely observed for the rest of the elements in the periodic table. Consequently, Pb(II) coordination chemistry is incredibly diverse and, so far, difficult to anticipate, yielding frequently unusual structures with new and interesting characteristics. Its relatively large ionic radius allows for the attainment of high coordination numbers, favoring the formation of polynuclear and polymeric species, although low coordination numbers can also sometimes be observed [10]. The rather unpredictable coordination geometry adopted by Pb(II) in different species can be correlated to the $6s^2$ lone pair stereoactivity, which explains its tendency to exhibit a hemidirected coordination geometry, with all the covalent bonds being concentrated on one hemisphere of the coordination sphere.

Carboxylate ligands are highly complementary towards Pb(II) due to the oxophilic nature of this cation. The coordination chemistry of Pb(II) carboxylates is a currently an active area of research, again based on the diverse modes of bonding of this metal. In such complexes, a wide range of coordination numbers for Pb(II) has been reported [11,12]. Benzoates are a subset of carboxylates, which are particularly interesting because their properties can be tuned based on proper substituent choice. The effect of substituents on the crystal structure of benzoates has been previously established for transition metals [13] and lanthanide complexes [14], and for some main-group elements including Pb [15]. An increased influence is expected for substituents with a strong ability to coordinate the metal (e.g., sulphonate or amine), but is unforeseen when only weak interactions are feasible (e.g., ether-type oxygen, including dioxolanes). Effects are unpredictable for substituents in which only steric effects are anticipated (e.g., the replacement of hydrogen with a simple methyl). Besides the Pb(II) flexible coordination sphere, carboxylate ligands also show a great variability in their coordination with different cations, ranging from monodentate to bridges between three metal centers. The combination of two flexible elements explains the fact that the crystal structure of Pb(II) complexes with benzoate derivatives are especially sensitive to small modifications to substituents in the ligand. For example, while [Pb(benzoate)$_2$(H$_2$O)] shows a 2D coordination polymer (CP) structure, the modification of the benzoate ligand with one methyl group in [Pb(2-methylbenzoate)$_2$(H$_2$O)] [15] or [Pb(3-methylbenzoate)$_2$(H$_2$O)] [16] yielded a 1D CP. Finally, the obtained structure can also be influenced by the inclusion of solvent molecules, often coordinated to Pb(II), and their nature. For instance, the exchange of the two methanol molecules in [Pb(2-methoxybenzoate)$_2$(MeOH)$_2$] by one aquo ligand in [Pb(2-methoxybenzoate)$_2$(H$_2$O)] resulted in the switch from a 1D to 2D CP [14]. The influence of the coordinating solvent was also evidenced by comparing the structures of [Pb(4-nitrobenzoate)$_2$] and [Pb(4-nitrobenzoate)$_2$(H$_2$O)$_2$] [17,18], in which the anhydrous compound was a 1D CP, while the two-hydrate compound showed a molecular structure. In general, the increase in the number of solvent molecules favors structures with reduced dimensionality.

The analysis of the crystal structures of compounds involving Pb-O interactions, with a wide range of lengths, is challenging. In the literature, different criteria modes can be found to classify these interactions, defined as either strong for clearly covalent bonds (or describing the primary coordination sphere) or weaker (or describing the second coordination sphere). As an approximation, 2.70 Å has been proposed as the limiting value for considering strong interactions, while weak interactions last up to 3.30 Å [11]. However, sometimes the values of Pb-O distances do not enter any of the gaps defined to categorize the interaction as strong or weak. Other authors have determined the type of Pb-O bonds by performing a valence sum analysis for each lead center [19,20]. Recently, a limit of 2.78 Å has been proposed for covalent bonds, while longer distances are attributed to the existence of tetrel bonds [21]. In fact, tetrel interactions are crucial to understand Pb(II) coordination chemistry [22].

All these idiosyncrasies trigger great interest in the coordination chemistry of Pb(II). Following our previous studies on the synthesis of coordination compounds based on benzoate derivatives [23–27], in this work, six new Pb(II) benzoate derivatives are prepared. In particular, we study three different benzoic acid derivatives with substituents containing ether-type oxygen atoms, either in a methoxy group located in the *para* position (2-methoxybenzoic) or as a ring incorporating two oxygen atoms connected to the aromatic ring for the 1,4-benzodioxan-5-carboxylic and piperonylic acid (Scheme 1). Reactions were performed under atmospheric pressure, and most of them were also performed at room temperature. The obtained results increase the understanding of the role of substituents in the structure of several CPs involving benzoate derivatives, as well as the effect of incorporating solvent molecules as ancillary ligands.
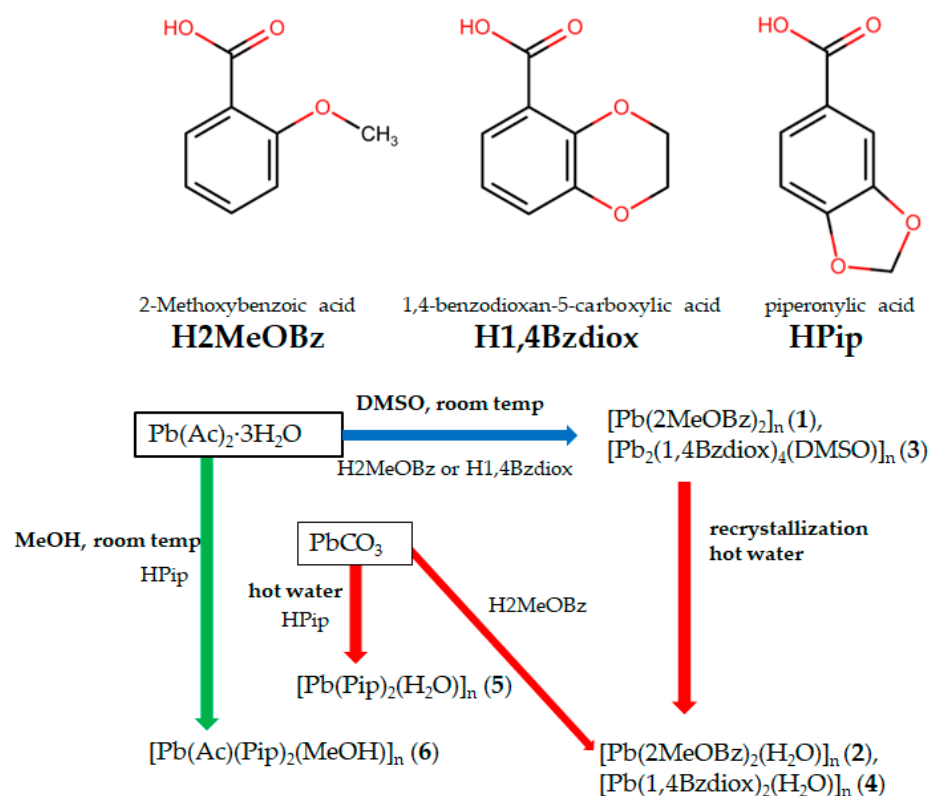
Scheme 1. Chemical structure of the ligands and synthetic pathway used in this work.

2. Results and Discussion

The six synthetized new compounds were all prepared in an open atmosphere. Compounds **1**, **3,** and **6** were obtained at room temperature in an organic solvent, either DMSO or MeOH, in which the respective precursors were soluble. Only compounds **2** and **4**, obtained via water recrystallization, and **5**, synthetized in water, needed to be heated to boiling to promote the dissolution of the precursor complex or to favor the reaction of the carbonate, respectively. The Pb(II) new coordination polymers are presented, grouping the compounds in two groups, related to benzoate (**1** to **4**) or piperonylate (**5** and **6**) ligands.

2.1. Pb(II) Complexes Containing 2MeOBz or 1,4Bzdiox Ligands

For each of the two studied benzoate derivatives, 2-methoxybenzoic and 1,4-benzodioxan-5-carboxylic acid, two different compounds were isolated, four with a crystalline nature, as indicated by the recorded powder XRD patterns (Figure 1). The distinctive patterns indicated that four different structures were obtained according to the synthetic conditions and/or incorporated solvent. Compounds $[Pb(2MeOBz)_2]_n$ (**1**) and $[Pb_2(1,4Bzdiox)_4(DMSO)]_n$ (**3**) were obtained in DMSO through the reaction of Pb(II) acetate with the acids. Compounds $[Pb(2MeOBz)_2(H_2O)]_n$ (**2**) and $[Pb(1,4Bzdiox)_2(H_2O)]_n$ (**4**) were obtained via the recrystallization in boiling water of **1** and **3**, respectively. For the four synthetized compounds, the elemental analysis data match well with the assigned stoichiometric composition. The precipitated compounds were further characterized using ATR-FTIR spectroscopy and compared with the free acids (Figures S1 and S2). The obtained spectra showed that the band assigned to the carboxylic acid group in the free acid (strong bands around 1670–1690 cm^{-1}) disappeared for the complexes, which implies the deprotonation of the acid and the formation of carboxylate. The four compounds displayed several carboxylate bands in the region of 1600–1434 cm^{-1}, indicating that the formation of several coordination modes for the carboxylate–Pb(II) bond occurs in each material. This observation could be confirmed in this work for compounds with an elucidated structure, and has already been described for other Pb(II) benzoate complexes. With regard to the

solvent, **2** and **4** showed a broad band between 3424 and 3384 cm^{-1}, attributed to the ν(O-H)$_{aqua}$ of water, while for **3**, the band allocated to ν(S=O) in DMSO was observed at 1003 cm^{-1}, together with the ν(C-S) vibration band at 727 cm^{-1} [28]. This characterization denotes that the use of water as a solvent induced the incorporation of solvent molecules in the final product. For synthesis performed in DMSO, the presence of the solvent in the structure was observed for **3**, but not for **1**.
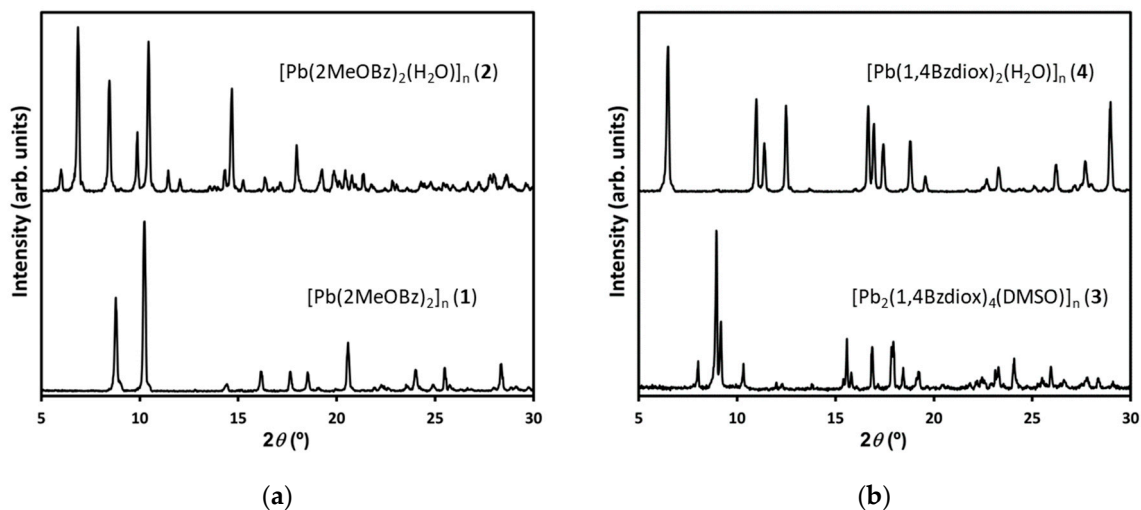
Figure 1. Comparison of powder XRD patterns collected at room temperature for samples (**a**) **1** and **2** involving 2-methoxy benzoic acid, and (**b**) **3** and **4** involving 1,4-benzodioxan-5-carboxylic acid.

By recrystallizing **1** in water, large crystals of [Pb(2MeOBz)$_2$(H$_2$O)]$_n$ (**2**) were formed, with enough quality to elucidate its crystal structure using XRD synchrotron radiation. The obtained data at 100K point to compound **2** belonging to the orthorhombic P2$_1$2$_1$2$_1$ space group (Table S1). The asymmetric unit contains two independent Pb(II) cations, four independent 2MeOBz ligands, and two aqua ligands. Each Pb(II) is coordinated by three oxygen atoms from two chelating carboxylate groups and one aqua ligand, with this Pb-O bond's length being in the range of 2.42–2.72 Å (Table S2). The coordination of each Pb(II) is completed with an oxygen atom of bridging carboxylate groups, e.g., Pb(1)-O(1) with 2.804(6) Å. As a consequence, the three first lengths of the four Pb-O bonds are in the range of conventional Pb-O bonds, but the later corresponds to a bond that can be considered as a tetrel interaction (Figure 2). Furthermore, the two independent Pb(II) atoms present a hemidirected coordination, facilitated by the stereochemical activity of a Pb(II) lone pair [29], which facilitates additional interaction with the oxygens in the methoxy groups via additional intramolecular tetrel bonds, e.g., Pb(1)···O(9) 3.062(7) Å and Pb(2)···O(11) 3.077(7) Å. The four independent 2MeOBz ligands show three different coordination modes, two of them with a chelating coordination mode, thus only interacting with a Pb(II) cation, one presenting a $\mu_3,\eta^1:\eta^2:\eta^1$ bridging mode, and four displaying a $\mu_2,\eta^1:\eta^2$ bridging mode, although also establishing an additional elongated Pb(1)-O(1) tetrel bond. These bridges define chains parallel to the *a* axis (Figure 3a). The presence of the aqua ligands determines a non-symmetric distribution of the phenyl rings with respect to the chain axis (Figure 3b). Only the methoxy group in the 2MeOBz ligand, in which the carboxylate group has bridging coordination, interacts with the Pb(II) through Pb···O tetrel interactions. Contrarily, for the ligands with a chelating carboxylate group, the disposition of the methoxy group prevents their participation in additional interactions (Figure 3c,d).
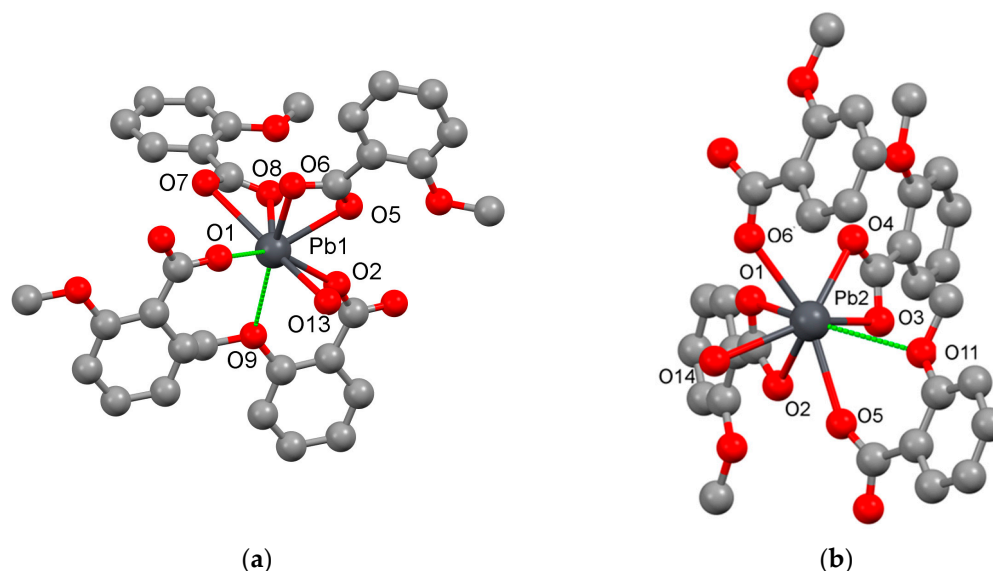
Figure 2. Coordination sphere of (**a**) Pb(1) and (**b**) Pb(2). Hydrogen atoms are omitted for clarity. Interactions with Pb-O distances longer than 2.74 Å are indicated with light-green sticks. Color codes: dark gray (Pb), red (O), gray (C).

The resolution of the crystal structure of **2** from the XRD single-crystal data, recorded at 100 K in the synchrotron (XALOC beamline), needs corroboration, since A-type alerts appeared in the check file related to residual electronic density close to the heavy Pb(II) atom, as well as insufficient absorption correction. Hence, the structure of **2** was also elucidated from data measured in the high-resolution powder XRD end station (MSPD beamline), using different wavelengths and temperatures (295 K) and proper absorption correction. The results are presented in Tables S1 and S3. The obtained crystallographic parameters for the single crystal and the powder were mainly coincident (compare data in Table S1), with only logical minor variations due to the different temperature used for the measurement. As a consequence, the crystal structure elucidated for **2** from the single crystal is considered as reliable. Furthermore, the XRD pattern of the bulk powder match those simulated from the structural data (Figure S3).

Contrarily to **2**, high-quality single crystals of [Pb(1,4Bzdiox)$_2$(H$_2$O)]$_n$ (**4**) could not be obtained after the recrystallization of **3** in water. In this case, the crystal structure resolution was attempted using powder XRD synchrotron radiation at 295 K. The preliminary results, however, showed short contacts affecting the hydrogen atoms of one ethylene group of the dioxolane ring, due to the difficulty of parametrizing probable disorder in this part of the ligand. Unfortunately, as the structure contains the heavy-atom Pb(II), the complete elucidation of this disorder in this flexible group of the ligand was not possible from the powder XRD data. Nevertheless, the coordination mode of Pb(II) and the structure of the unit cell were not affected by the disorder; the Rietveld fit is satisfactory (Figure S4). Briefly, the key structural points are that **4** belongs to the orthorhombic I *b a* 2 space group. Like **2**, this compound consists of a 1D coordination polymer, in which 1,4Bzdiox ligands show diverse coordination modes to Pb(II) (μ_1,η^2-chelating and μ_2,η^1:η^2-bridging modes). Finally, one oxygen atom of each dioxane group establishes a tetrel bond with the metal cation (Figures S5 and S6).
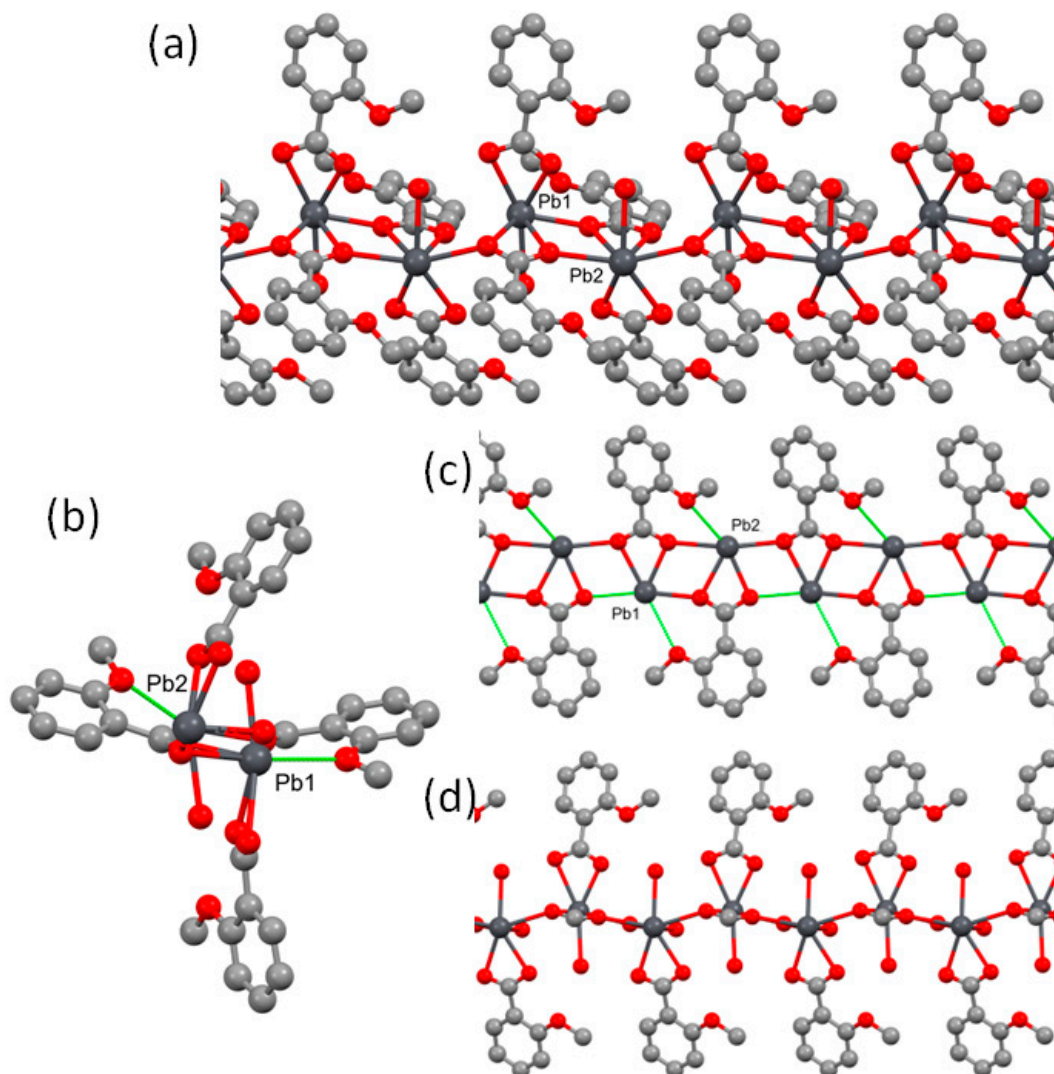
Figure 3. Crystal structure of compound **2**: (**a**) chain view along *c* axis, (**b**) chain view along *a* axis, and (**c**,**d**) simplified pictures showing only half of the 2MeOBz ligands to emphasize their different role. In (**b**–**d**), hydrogen atoms are omitted for clarity. Color codes: dark gray (Pb), red (O), gray (C), white (H).

Solid samples of the prepared compounds **1** to **4** were observed under black light by using a set of commercially available 8 W black-light tubes, with a spectral peak centered around 365 nm. Among the described new Pb(II) benzoate family of compounds, only two, **2** and **4**, showed a moderate blue photoluminescence visible to the naked eye. In contrast, **1** and **3** did not show the photoluminescence property. Photoluminescence was only observed in the solid state, which indicates that a fixed position for the metal centers and ligands is a requisite for this property to be noticeable. The polymeric structure was broken in solution by incorporating additional solvent molecules in the sphere of coordination of Pb(II). The compound [Pb(2MeOBz)$_2$(H$_2$O)]$_n$ (**2**) was obtained as large crystalline needles, giving a different photoluminescence spectrum as a function of the needle orientation (walls emit a greenish light, whereas tips emit in orange color) (Figure 4a). Compound [Pb(1,4Bzdiox)$_2$(H$_2$O)]$_n$ (**4**) also precipitated as needles, but they were to fine to separate the measurement as a function of the orientation. Globally, the sample showed a moderate greenish yellow photoluminescence (Figure 4b). It is worth mentioning that a given combination of Pb(II) and a benzoate derivative is not enough to produce a photoluminescent polymer, as demonstrated in this work. It is reasoned that the condition to obtain a material showing photoluminescence is particularly related to symmetry, as

the only two compounds that show this property in this study, **2** and **4**, crystallize in non-centrosymmetric space groups.
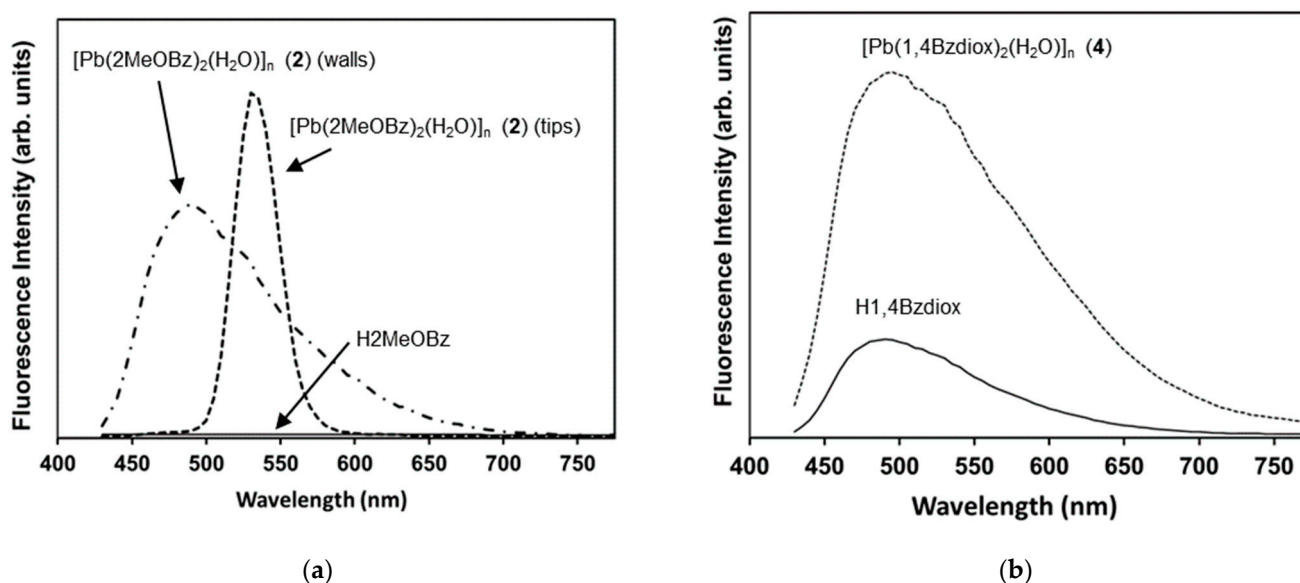

Figure 4. Spectral profiles representing photoluminescence intensity versus emission wavelength in the 415–750 nm range for (**a**) [Pb(2MeOBz)$_2$(H$_2$O)]$_n$ (**2**) needles (1 for the tips, 2 for the walls, and 3 for H2MeOBz acid); (**b**) 1 for [Pb(1,4Bzdiox)$_2$(H$_2$O)]$_n$ (**4**) and 2 for H1,4Bzdiox acid.

2.2. Pb(II) Complexes Containing Piperonylate Ligand

As described for the benzoate derivatives, the product of the reaction between Pb(II) acetate and piperonylic acid also depended on the used experimental conditions. Two different compounds were generated, as demonstrated in the powder XRD analysis (Figures S7 and S8). The reaction of the precursors in hot water allowed the exchange of both acetate ligands by piperonylate, yielding compound [Pb(Pip)$_2$(H$_2$O)]$_n$ (**5**). When the solvent was methanol, a mixed acetate piperonylate complex, [Pb(Ac)(Pip)$_2$(MeOH)]$_n$ (**6**), was formed at room temperature. The elemental analysis of **5** matches the expected formula for this compound. On the contrary, the measured data for **6** strongly suggest that MeOH is partially interchanged with water by exposing the sample to ambient air. As for the benzoate compounds, the ATR-FTIR spectra of **5** and **6** showed that the band of the free carboxylic acid group (in the region of 1670–1700 cm^{-1}) disappears for the complexes due to the deprotonation and formation of carboxylate (Figure S9). Furthermore, **5** displayed a broad band attributed to ν(O-H)$_{aqua}$ (3424–3384 cm^{-1}), while for **6,** the solvent band attributed to ν(OH)$_{MeOH}$ appeared at 3363 cm^{-1} [30], perhaps with some water contribution due to the interchange of MeOH with water upon air exposure.

For **5**, it was not possible to obtain crystals of enough quality to allow us to elucidate its crystal structure. However, the powder XRD pattern of this compound is reasonably similar to the pattern of the reported [Cd(Pip)$_2$(H$_2$O)]$_n$ 1D coordination polymer [23] (Figure S7). This cadmium complex has the same stoichiometry as **5**, and a similar ATR-FTIR spectrum. All these observations indicated that both compounds must have a comparable structure, thus indicating a 1D coordination polymer structure for **5**.

Compound **6** precipitated forming crystals with enough size and quality to elucidate its structure via XRD synchrotron radiation at 100 K (Tables S5 and S6). This compound crystalizes in the monoclinic P2$_1$/c space group. The asymmetric unit contains only one Pb(II) cation, one Pip, and one acetate ligand, together with one methanol coordinated by the oxygen atom (Figure 5). Considering Pb-O bond lengths in the range of 2.40–2.72 Å, the coordination number of the metal center, which is six, includes all the Pb-O$_{acetate}$ bonds, with the acetate showing a $\mu_2,\eta^2{:}\eta^2$-bridging mode, the Pb-O$_{MeOH}$ bond, and only one

Pb-O bond with the carboxylate of the Pip ligand, Pb-O(3)$_{Pip}$ (Figure 6). The hemidirected coordination sphere of Pb(II), considering these strong bonds, reflects the stereochemical activity of the metal lone electron pair [29]. The expansion of these bonds generates chains parallel to the *c* axis. Moreover, the other oxygen of the carboxylate group of the Pip ligand shows two additional Pb-O$_{Pip}$ elongated bonds. One bond, Pb-O(3)$_{Pip}$ 2.796(9) Å, reinforces the chain structure, but the other, Pb'-O(4)$_{Pip}$ 2.84(1), connects neighboring chains into a 2D network parallel to the *ac* plane. Thus, considering these additional Pb-O bonds, Pip ligands show a $\mu_2,\eta^1:\eta^2$-bridging mode. This structure can be envisaged as encompassing 1D chains, with Pb(II) centers showing hemidirected coordination, that are further arranged into a 2D supramolecular structure by additional Pb-O tetrel bonds (Figure 7). In the packing, the protruding Pip ligands interdigitate, favoring weak interlayer contacts through Pip ligands of adjacent layers. Although there are some small discrepancies between the measured powder XRD pattern and the pattern simulated from the single-crystal data (Figure S8), these can be justified by taking into account the lability of the MeOH ligand and its probable interchange with water on exposure to the atmosphere, which also caused some minor inconsistencies in the elemental analysis of the sample, as described previously. For this sample, single crystals were preserved in their mother liqueur until XRD characterization to assure its quality, while the bulk powder was stored in dry conditions in an open atmosphere.
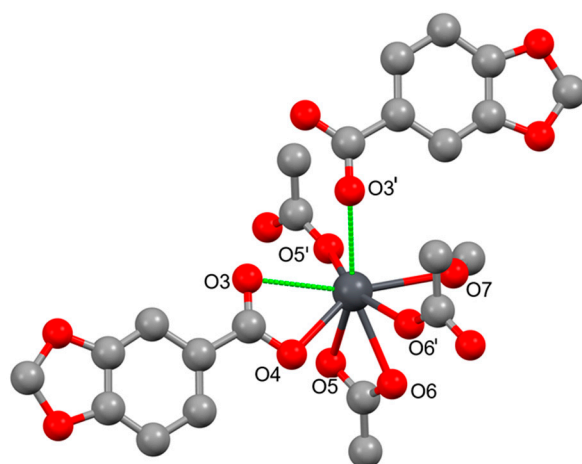
Figure 5. Coordination sphere of Pb(II) in **6**. Interactions with Pb-O distances greater than 2.74 Å are indicated with light-green sticks. Color codes: dark gray (Pb), red (O), gray (C).
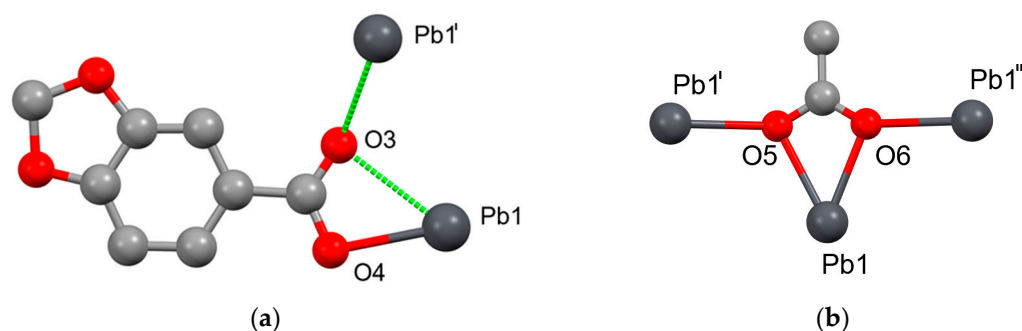

Figure 6. Coordination modes of (**a**) the carboxylate group of Pip and (**b**) acetate ligands in **6**. Interactions with Pb-O distances greater than 2.74 Å are indicated as light-green sticks. Color codes: dark gray (Pb), red (O), gray (C).
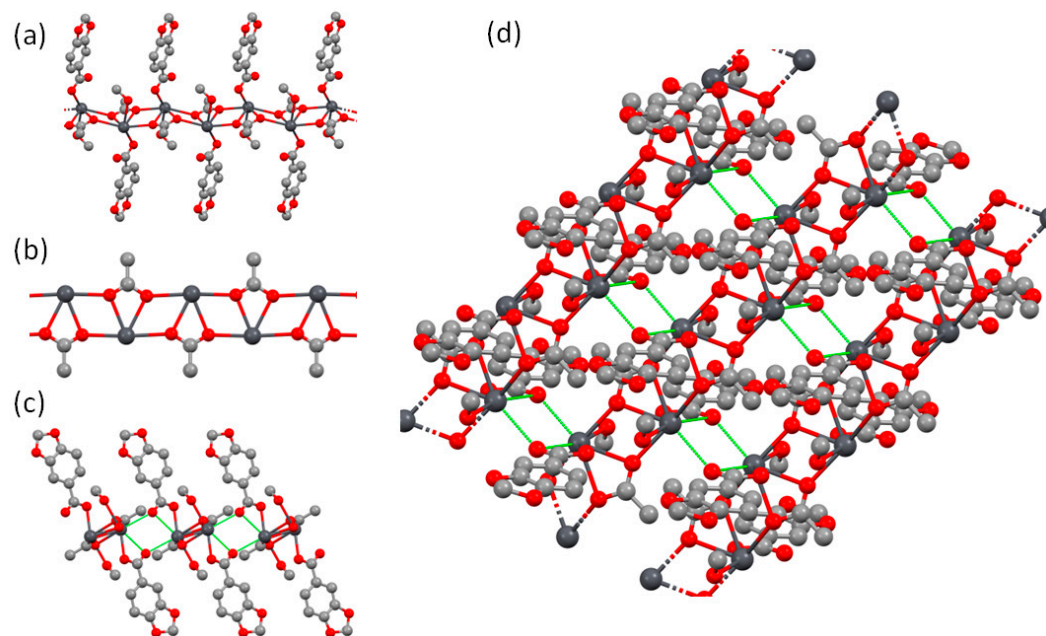
Figure 7. Crystal structure of 6. Note that without considering the tetrel bonds (green sticks), the compound is a 1D coordination polymer (**a**,**b**). Tetrel bonds arrange the chains into a 2D supramolecular network (**c**,**d**). Color codes: dark gray (Pb), red (O), gray (C).

The two compounds with HPip acid do not showed luminescence. Although they contain water molecules, these compounds crystallize in centrosymmetric space groups. Hence, these results reinforce our suggestion that photoluminescence is associated with non-centrosymmetric space groups.

3. Experimental

3.1. Materials and Methods

Either lead(II) acetate trihydrate ($Pb(Ac)_2 \cdot 3H_2O$ or lead(II) carbonate ($PbCO_3$)) was used as the metal source. 2-Methoxybenzoic (H2MeOBz), 1,4-benzodioxan-5-carboxylic (H1,4Bzdiox), and piperonylic (HPip) acids were used as the ligand precursors. The mentioned reagents and organic solvents (dimethylsulfoxide, DMSO; methanol, MeOH) were all purchased from Sigma Aldrich (Merck KGaA, Darmstadt, Germany). Water was purified in a Millipore Milli-Q system. Powder X-ray diffraction (XRD) patterns were measured at room temperature in a Siemens D5000 apparatus (Siemens now Bruker, Karlsruhe, Germany), using CuK_α radiation. Patterns were recorded from 2θ = 5 to 30°, with a step scan of 0.02° counting for 1 s at each step. Fourier transform infrared (FTIR) spectra were recorded in a Tensor 27 (Bruker, Ettlingen, Germany) spectrometer, equipped with an attenuated total reflectance (ATR) MKII Golden Gate, with a diamond window in the range of 600–4000 cm^{-1}. The photoluminescence properties of the selected samples were studied via confocal scanning laser microscopy (CSLM, Leica TCS SP5). Previously, ca. 20 mg of the powder sample were mounted on Ibidi culture dishes (Ibidi GmbH, Martinsried, Germany) and excited with a blue diode laser (405 nm). The fluorescence intensity was recorded, generating a lambda stack, with an emission wavelength ranging from 415 to 750 nm.

3.2. Synthesis and Basic Characterization

[Pb(2MeOBz)$_2$]$_n$ (**1**): A solution containing H2MeOBz (304 mg, 2.00 mmol) in DMSO (15 mL) was added to a solution of $Pb(Ac)_2 \cdot 3H_2O$ (380 mg, 1.00 mmol) in DMSO (25 mL). The resulting colorless solution was slowly concentrated via evaporation until **1** was precipitated. The obtained solid was filtered and washed with DMSO (5 mL) and dried under air flow. The entire process was carried out at room temperature. Yield: 386 mg

(76%). Anal. Calc. for $C_{16}H_{14}O_6Pb$ (509.48 gmol^{-1}): C, 37.72; H, 2.77. Found: C, 37.99; H, 2.79%. ATR-FTIR (wavenumber, cm^{-1}): 2839(w), 1600(s), 1584(s), 1507(s), 1437(m), 1382(s), 1294(m), 1273(m), 1236(s), 1159(s), 1101(m), 1049(m), 1007(m), 955(w), 862(s), 787(m), 756(s), 705(m), 661(s).

[Pb(2MeOBz)$_2$(H$_2$O)]$_n$ (**2**): This compound was obtained via the recrystallization of **1**; 250 mg of **1** was dissolved in 200 mL of boiling water and, after cooling to room temperature, crystalline needles of **2** were precipitated. Yield: 198 mg (82%). Anal. Calc. for $C_{16}H_{16}O_7Pb$ (527.50 gmol^{-1}): C, 36.43; H, 3.06. Found: C, 36.72; H, 2.97%. ATR-FTIR (wavenumber, cm^{-1}): 3504(w), 3407(w), 2938(w), 2835(w), 1600(m), 1582(m), 1508(m), 1486(m), 1434(m), 1379(s), 1292(m), 1273(m), 1243(s), 1184(m), 1161(m), 1102(m), 1049(m), 1019(s), 950(w), 869(s), 859(s), 852(s), 788(m), 757(s), 705(m), 662(s). Alternatively, the same compound can be prepared from PbCO$_3$ and H2MeOBz via a reaction in boiling water.

[Pb$_2$(1,4Bzdiox)$_4$(DMSO)]$_n$ (**3**): A solution containing H14Bzdiox (361 mg, 2.00 mmol) in DMSO (15 mL) was added to a solution of Pb(Ac)$_2$·3H$_2$O (380 mg, 1.00 mmol) in DMSO (25 mL). The resulting colorless solution was slowly concentrated via evaporation until **3** was precipitated. The obtained solid was filtered and washed with DMSO (5 mL) and dried under air flow. The entire process was carried out at room temperature. Yield: 347 mg (57%). Anal. Calc. for $C_{38}H_{34}O_{17}Pb_2S$ (1209.13 gmol^{-1}): C, 37.75; H, 2.83. Found: C, 37.89; H, 2.77. ATR-FTIR (wavenumber, cm^{-1}): 2870(w), 1600(w), 1566(m), 1537(s), 1461(m), 1447(m), 1381(s), 1351(s), 1304(m), 1280(s), 1256(m), 1241(m), 1218(s), 1184(m), 1086(s), 1045(m), 1003(s) (DMSO), 952(m), 920(w), 886(m), 821(s), 770(m), 748(m), 727(w) DMSO, 716(m), 654(w), 611(w).

[Pb(1,4Bzdiox)$_2$(H$_2$O)]$_n$ (**4**): This compound was obtained via the recrystallization of **3**; 300 mg of **3** were dissolved in 200 mL of boiling water and, after cooling and standing to room temperature, needles of **4** were precipitated. Yield: 53 mg (87%). Anal. Calc. for $C_{18}H_{16}O_9Pb$ (583.51 gmol^{-1}): C, 37.05; H, 2.76. Found: C, 37.21; H, 2.66%. ATR-FTIR (wavenumber, cm^{-1}): 3422(w), 2927(w), 2873(w), 1598(m), 1536(s), 1511(s), 1464(m), 1446(m), 1387(s), 1302(m), 1281(m), 1250(m), 1212(m), 1187(m), 1085(m), 1044(m), 957(w), 921(m), 886(m), 823(s), 758(s), 721(m), 655(w), 606(w).

[Pb(Pip)$_2$(H$_2$O)]$_n$ (**5**): PbCO$_3$ powder (300 mg, 1.12 mmol) was added to a solution containing HPip (332 mg, 2.00 mmol) in water (150 mL). The reaction mixture was boiled for one hour, and then the undissolved excess of PbCO$_3$ was filtered. After cooling, the resulting solution to room temperature, **1** was precipitated as a white solid, which was filtered and washed with water three times (5 mL) and, finally, dried in air. Yield: 348 mg (63%). Anal. Calc. for $C_{16}H_{12}O_9Pb$ (555.46 gmol^{-1}): C, 34.60; H, 2.18. Found: C, 34.79; H, 2.00%. ATR-FTIR (wavenumber, cm^{-1}): 3218(w), 2906 (w), 1652(w), 1628(w), 1604(w), 1503(s), 1433(s), 1381(s), 1350(m), 1258(m), 1242(s), 1168(w), 1113(m), 1074(w), 1040(s), 935(m), 919(w), 888(w), 820(m), 804(m), 773(s), 721(w), 681(m).

[Pb(Ac)(Pip)(MeOH)]$_n$ (**6**): A solution of HPip (166 mg, 1.00 mmol) in MeOH (40 mL) was added to a solution of Pb(Ac)$_2$·3H$_2$O (380 mg, 1.00 mmol) in MeOH (25 mL). The resulting colorless solution was slowly concentrated via evaporation until crystals of **6** were precipitated, which were filtered and washed with cold methanol (5 mL) and dried in air. The entire process was carried out at room temperature. Yield: 224 mg (48%). Anal. Calc. for $C_{11}H_{12}O_7Pb$ (463.41 gmol^{-1}): C, 28.51; H, 2.61. Anal. Calc. considering that 65% of MeOH was substituted with H$_2$O, $C_{10.35}H_{10.7}O_7Pb$ (454.29 gmol^{-1}): C, 26.83; H, 2.33. Found: C, 26.70; H, 2.14%). ATR-FTIR (wavenumber, cm^{-1}): 3363(m), 2908 (w), 1650(w), 1627(w), 1609(w), 1526 (s), 1504(s), 1430(s), 1369(m), 1331(s), 1256(s), 1240(s), 1168(m), 1110(m), 1073(w), 1034(s), 1010(m), 937(w), 918(s), 889(w), 823(m), 806(m), 767(s), 720(w), 682(s), 605(m). For structure determination, the crystals were kept in the mother solution until just before X-ray diffraction data acquisition.

3.3. X-ray Crystallographic Data

The crystal structures of **2** and **6** were determined using synchrotron single-crystal XRD data that were collected in the XALOC beamline at the ALBA Synchrotron (Cerdanyola del

Valles, Spain) [31]. Data acquisition was performed at 100 K with a 0.72932 Å wavelength using the Dectris Pilatus 6M detector placed 120 mm from the sample. Three sets of 360° φ-scans (in steps of 0.5° and 0.15 s·step^{-1}) at three κ angles (0°, 45°, and 90°) were attempted, and the successful ones were merged to increase data completeness and redundancy. Data were indexed, integrated, and scaled using the XDS software [32]. The crystal structures were determined via intrinsic phasing and refined with SHELXL using the full-matrix least-squares methods on F^2 (version 2014/7) [33], using Olex2 as the graphical interface [34]. Hydrogen atoms bonded to carbon atoms were placed in calculated positions, with isotropic displacement parameters fixed at 1.2 times the U$_{eq}$ of the corresponding carbon atoms. Data for compound **2** were also taken at room temperature using Mo Kα radiation (k = 0.71073 Å) in a SMART-APEX diffractometer with a CCD detector (Bruker AXS Inc., Madison, WI, USA). An empirical absorption correction was applied (SADABS), solved, and refined using the same procedure described previously.

Furthermore, the structure elucidation of **4** was attempted with synchrotron powder XRD analysis, carried out in a high-resolution powder diffraction end station of the MSPD beamline (BL04) at 295 K at the ALBA synchrotron [35]. The samples were measured in transmission mode, in a 0.7 mm glass capillary, at 295 K, with an SR-XRPD energy of 30 keV (0.49603 Å wavelength determined from a Si NIST-640d reference). The Mythen-II detector (six modules, 1280 channels/module, 50 μm/channel, sample-to-detector distance of 550 mm) was used. The powder diffraction pattern was indexed using DICVOL04 (M20 = 31.5 F20 = 207.9) [36], obtaining a orthorhombic cell for **4**, with the systematic absences being consistent with an I-centered lattice (I *b a* 2 space group). The crystal structure was determined using the direct-space methodology implemented in the DA-JUST [37] and TALP [38] software, introducing, as the initial model, two molecules of the 1,4-benzodioxane ligand, and as rigid bodies, one Pb atom and one water molecule. A restrained Rietveld refinement of the candidate solution yielded the final crystal structure (R$_{wp}$ = 0.145). Refined parameters: 83 atomic coordinates, B$_{iso-overall}$, B$_{iso-Pb}$, 3 cell parameters, 3 pseudo-Voigt coefficients, zero-shift, and scale factor. Restraints: bond distances, angles, and plane restraints only for the 1,4-benzodioxane molecules. The H atoms were placed at calculated positions.

The CCDC (numbers 2300681 (**2**, 100 K), 2300682 (**2**, r.t.), 2300680 (**4**, 100 K), and 2300683 (**6**, 100 K) respectively) contains the supplementary crystallographic data for this paper. These data can be obtained free of charge via https://www.ccdc.cam.ac.uk/structures/?l (or from the CCDC, 12 Union Road, Cambridge CB2 1EZ, UK; Fax: +44 1223 336033; E-mail: deposit@ccdc.cam.ac.uk). Crystal data and relevant details of the structure refinement for compounds **2** and **6** are reported in Tables S1–S6 of the Supplementary Information. Molecular graphics were generated with the Mercury 4.0 program [39].

4. Conclusions

Six new coordination Pb(II) complexes involving three different ligands, all derived from benzoic acid and incorporating substituents with ether-type oxygen, were prepared under soft experimental conditions. Two new materials were isolated for each ligand. The used solvent, water, DMSO, or MeOH, was the main parameter determining the nature of the isolated polymer. The use of water as the solvent promoted the inclusion of aqua ligands in the crystalized products involving 2-metoxybenzoate, 1,4-benzodioxan-5-carboxylate ligands. These aqua ligands determined the formation of luminescent materials. In contrast, compounds with the same benzoate derivative but prepared in an organic solvent (DMSO) did not show this property. In contrast, the piperonylate coordination polymer obtained in water did not display photoluminescence. In this case, by changing the solvent to methanol, a mixed acetate–piperonylate compound was obtained. In the crystal structure of these compounds, tetrel bonds play a crucial role to organize the polymeric chains and to extend the structure in two dimensions.

References

1. Magyar, J.S.; Weng, T.-C.; Stern, C.M.; Dye, D.F.; Rous, B.W.; Payne, J.C.; Bridgewater, B.M.; Mijovilovich, A.; Parkin, G.; Zaleski, J.M.; et al. Reexamination of Lead(II) Coordination Preferences in Sulfur-Rich Sites: Implications for a Critical Mechanism of Lead Poisoning. *J. Am. Chem. Soc.* **2005**, *127*, 9495–9505. [CrossRef]
2. Yang, J.; Ma, J.-F.; Liu, Y.-Y.; Ma, J.-C.; Batten, S.R. A Series of Lead(II) Complexes with Π−π Stackings: Structural Diversities by Varying the Ligands. *Cryst. Growth Des.* **2009**, *9*, 1894–1911. [CrossRef]
3. Zhang, H.; Yan, Z.-A.; Wu, Z.-M.; Lin, Z.-Q.; Liao, W.-M.; He, J. Hydrated Proton Conduction and Luminescence of a Carboxylate and Sulfonate-Included Lead(II) Coordination Polymer. *J. Solid State Chem.* **2020**, *287*, 121325. [CrossRef]
4. Qi, H.-X.; Jo, H.; Ok, K.M. Pb[NC₅H₃(CO₂)₂]: A White Light Emitting Single Component Coordination Polymer Revealing High Quantum Efficiency and Thermal Stability. *Inorg. Chem. Front.* **2018**, *5*, 1273–1276. [CrossRef]
5. Barszcz, B.; Masternak, J.; Kowalik, M. Structural Insights into Coordination Polymers Based on 6s2 Pb(II) and Bi(III) Centres Connected via Heteroaromatic Carboxylate Linkers and Their Potential Applications. *Coord. Chem. Rev.* **2021**, *443*, 213935. [CrossRef]
6. Shen, W.; Chen, J.; Wu, J.; Li, X.; Zeng, H. Nonlinear Optics in Lead Halide Perovskites: Mechanisms and Applications. *ACS Photonics* **2021**, *8*, 113–124. [CrossRef]

7. Sui, B.; Zhao, W.; Ma, G.; Okamura, T.; Fan, J.; Li, Y.-Z.; Tang, S.-H.; Sun, W.-Y.; Ueyama, N. Novel Pb(Ii) Coordination Frameworks: Synthesis, Crystal Structures and Unusual Third-Order Nonlinear Optical Properties. *J. Mater. Chem.* **2004**, *14*, 1631–1639. [CrossRef]

8. Saah, S.A.; Boadi, N.O.; Adu-Poku, D.; Wilkins, C. Lead Ethyl Dithiocarbamates: Efficient Single-Source Precursors to PbS Nanocubes. *R. Soc. Open Sci.* **2019**, *6*, 190943. [CrossRef]

9. Ezenwa, T.E.; McNaughter, P.D.; Raftery, J.; Lewis, D.J.; O'Brien, P. Full Compositional Control of PbS x Se 1−x Thin Films by the Use of Acylchalcogourato Lead(ii) Complexes as Precursors for AACVD. *Dalton Trans.* **2018**, *47*, 16938–16943. [CrossRef]

10. Claudio, E.S.; Godwin, H.A.; Magyar, J.S. Fundamental Coordination Chemistry, Environmental Chemistry, and Biochemistry of Lead(II). In *Progress in Inorganic Chemistry*; Karlin, K.D., Ed.; John Wiley & Sons, Inc.: New York, NY, USA, 2002; Volume 51, pp. 1–144; ISBN 978-0-471-26534-4.

11. Davidovich, R.L.; Stavila, V.; Marinin, D.V.; Voit, E.I.; Whitmire, K.H. Stereochemistry of Lead(II) Complexes with Oxygen Donor Ligands. *Coord. Chem. Rev.* **2009**, *253*, 1316–1352. [CrossRef]

12. Hu, M.-L.; Morsali, A.; Aboutorabi, L. Lead(II) Carboxylate Supramolecular Compounds: Coordination Modes, Structures and Nano-Structures Aspects. *Coord. Chem. Rev.* **2011**, *255*, 2821–2859. [CrossRef]

13. Rajakannu, P.; Kaleeswaran, D.; Banerjee, S.; Butcher, R.J.; Murugavel, R. Effect of Benzoic Acid Substituents and Additional Functional Groups of Ancillary Ligands in Modulating the Nuclearity and Aggregation Behavior of Transition Metal Carboxylates. *Inorg. Chim. Acta* **2019**, *486*, 283–293. [CrossRef]

14. Utochnikova, V.V.; Kalyakina, A.S.; Solodukhin, N.N.; Aslandukov, A.N. On the Structural Features of Substituted Lanthanide Benzoates. *Eur. J. Inorg. Chem.* **2019**, *2019*, 2320–2332. [CrossRef]

15. Sarma, R.; Baruah, J.B. Solvent Coordination in Changing Dimensionality of Lead Benzoate Coordination Polymers. *Inorganica Chim. Acta* **2009**, *362*, 4977–4984. [CrossRef]

16. Dai, J.; Yang, J.; An, X. *catena*-Poly[[aqua(3-methylbenzoato-κ²O, O')lead(II)]-μ-3-methylbenzoato-κ⁴O:O, O':O']. *Acta Crystallogr. E Struct. Rep. Online* **2009**, *65*, m709–m710. [CrossRef]

17. Baruah, J.B. *CCDC 673854: Experimental Crystal Structure Determination*; CCDC: Cambridge, UK, 2016. [CrossRef]

18. Usubaliev, B.T.; Amirov, A.S.; Amiraslanov, I.R.; Mamedov, K.S. Crystal and molecular structure of di(para-nitrobenzoato)diaquolead. *J. Struct. Chem.* **1989**, *30*, 851–853. [CrossRef]

19. Easterday, C.C.; Dedon, L.R.; Zeller, M.; Oertel, C.M. Helical ∞ 1 [Pb₂O] Chains in Polymorphs of Pb₂O(C₆H₅COO)₂. *Cryst. Growth Des.* **2014**, *14*, 2048–2055. [CrossRef]

20. Liu, E.E.; Gang, C.; Zeller, M.; Fabini, D.H.; Oertel, C.M. Ligand-Induced Variations in Symmetry and Structural Dimensionality of Lead Oxide Carboxylates. *Cryst. Growth Des.* **2017**, *17*, 1574–1582. [CrossRef]

21. Seth, S.K.; Bauzá, A.; Mahmoudi, G.; Stilinović, V.; López-Torres, E.; Zaragoza, G.; Keramidas, A.D.; Frontera, A. On the Importance of Pb··· X (X = O, N, S, Br) Tetrel Bonding Interactions in a Series of Tetra- and Hexa-Coordinated Pb(II) Compounds. *CrystEngComm* **2018**, *20*, 5033–5044. [CrossRef]

22. Bauzá, A.; Seth, S.K.; Frontera, A. Tetrel Bonding Interactions at Work: Impact on Tin and Lead Coordination Compounds. *Coord. Chem. Rev.* **2019**, *384*, 107–125. [CrossRef]

23. Ejarque, D.; Sánchez-Férez, F.; Ayllón, J.A.; Calvet, T.; Font-Bardia, M.; Pons, J. Diverse Structures and Dimensionalities in Zn(II), Cd(II), and Hg(II) Metal Complexes with Piperonylic Acid. *Cryst. Growth Des.* **2020**, *20*, 383–400. [CrossRef]

24. Guerrero, M.; Vázquez, S.; Ayllón, J.A.; Calvet, T.; Font-Bardia, M.; Pons, J. Zn(II) and Cd(II) Coordination Dimers Based on Mixed Benzodioxole-Carboxylate and N-Donor Ligands: Synthesis, Characterization, Crystal Structures and Photoluminescence Properties. *ChemistrySelect* **2017**, *2*, 632–639. [CrossRef]

25. Guerrero, M.; Pou, R.; Bayés-García, L.; Font-Bardia, M.; Sort, J.; Pons, J.; Ayllón, J.A. Syntheses, Supramolecular Architectures and Photoluminescence Properties of Zn(II) Complexes Based on 3,5 dihydroxybenzoic and Pyridine/Pyrazole Derived Ligands. *Inorg. Chem. Comm.* **2018**, *96*, 34–38. [CrossRef]

26. Soldevila-Sanmartín, J.; Ayllón, J.A.; Calvet, T.; Font-Bardia, M.; Domingo, C.; Pons, J. Synthesis, Crystal Structure Inorganic Chemistry Communications and Magnetic Properties of a Cu(II) Paddle-Wheel Complex with Mixed Bridges. *Inorg. Chem. Comm.* **2016**, *71*, 90–93. [CrossRef]

27. Sánchez-Férez, F.; Pou, R.; Bayés-García, L.; Font-Bardia, M.; Pons, J.; Ayllón, J.A. Benzoate Substituents Effects on the Structure of Zn(II) Complexes and 1D 4,4′-Bipyridine Derived Coordination Polymers. *Inorg. Chim. Acta* **2020**, *500*, 119218. [CrossRef]

28. Cotton, F.A.; Francis, R.; Horrocks, W.D. Sulfoxides as ligands II. The infrared spectra of some dimethyl sulfoxide complexes. *J. Phys. Chem.* **1960**, *64*, 1534–1536. [CrossRef]

29. Kowalik, M.; Masternak, J.; Brzeski, J.; Daszkiewicz, M.; Barszcz, B. Effect of a Lone Electron Pair and Tetrel Interactions on the Structure of Pb(II) CPs Constructed from Pyrimidine Carboxylates and Auxiliary Inorganic Ions. *Polyhedron* **2022**, *219*, 115818. [CrossRef]

30. Williams, D.H.; Fleming, I. *Spectroscopic Methods in Organic Chemistry*, 6th ed.; McGraw-Hill: London, UK, 2008; ISBN 978-0-07-711812-9.

31. Juanhuix, J.; Gil-Ortiz, F.; Cuní, G.; Colldelram, C.; Nicolás, J.; Lidón, J.; Boter, E.; Ruget, C.; Ferrer, S.; Benach, J. Developments in Optics and Performance at BL13-XALOC, the Macromolecular Crystallography Beamline at the Alba Synchrotron. *J. Synchrotron Rad.* **2014**, *21*, 679–689. [CrossRef]

32. Kabsch, W. XDS. *Acta Crystallogr. D Biol. Crystallogr.* **2010**, *66*, 125–132. [CrossRef]

33. Sheldrick, G.M. Crystal Structure Refinement with SHELXL. *Acta Crystallogr. C Struct. Chem.* **2015**, *71*, 3–8. [CrossRef]
34. Dolomanov, O.V.; Bourhis, L.J.; Gildea, R.J.; Howard, J.A.K.; Puschmann, H. OLEX2: A Complete Structure Solution, Refinement and Analysis Program. *J. Appl. Crystallogr.* **2009**, *42*, 339–341. [CrossRef]
35. Fauth, F.; Peral, I.; Popescu, C.; Knapp, M. The new Material Science Powder Diffraction beamline at ALBA Synchrotron. *Powder Diffr.* **2013**, *28*, S360–S370. [CrossRef]
36. Boultif, A.; Louër, D. Powder pattern indexing with the dichotomy method. *J. Appl. Crystallogr.* **2004**, *37*, 724–731. [CrossRef]
37. Vallcorba, O.; Rius, J.; Frontera, C.; Peral, I.; Miravitlles, C. DAJUST: A suite of computer programs for pattern matching, space-group determination and intensity extraction from powder diffraction data. *J. Appl. Crystallogr.* **2012**, *45*, 844–848. [CrossRef]
38. Vallcorba, O.; Rius, J.; Frontera, C.; Miravitlles, C. TALP: A multisolution direct-space strategy for solving molecular crystals from powder diffraction data based on restrained least squares. *J. Appl. Crystallogr.* **2012**, *45*, 1270–1277. [CrossRef]
39. Macrae, C.F.; Sovago, I.; Cottrell, S.J.; Galek, P.T.A.; McCabe, P.; Pidcock, E.; Platings, M.; Shields, G.P.; Stevens, J.S.; Towler, M.; et al. Mercury 4.0: From Visualization to Analysis, Design and Prediction. *J. Appl. Crystallogr.* **2020**, *53*, 226–235. [CrossRef]